3D numerical study of wet foam behavior and channels by MPS method

†Zhongguo Sun, * Yong Zhang, Qixin Liu, Yijie Sun and Guang Xi

School of Energy and Power Engineering, Xi'an Jiaotong University, China

*Presenting author: 2738700649@qq.com

†Corresponding author: sun.zg@xjtu.edu.cn

Abstract

Wet foam consists of many bubbles. Its geometry and mechanical property are complex. The contact between bubbles generates structure like porous media with Plateau channels, and the surface tension force acts on both sides of the liquid film. Seldom model or method can simulate the phenomenon of liquid foam in detail. In this study, the moving particle semi-implicit (MPS) method is employed to study wet foam behavior and channels. The Lagrangrian description and particles with flow information are applied, which has inherent advantages in dealing with large deformation of interface. A double gas-liquid interface surface tension model is studied based on the surface free energy model, and the interface tension was introduced to study the interaction between bubbles and solid wall. Further, the behavior of three-dimensional multiple bubbles is investigated in detail. The typical behavior of bubbles are analyzed. The effects of liquid viscosity, surface tension coefficient and bubble size on the behavior of bubbles are discussed. Subsequently, the forming process of different kinds of Plateau channel structure were displayed and discussed in detail.

Keywords: MPS method; double gas-liquid interface surface tension; interface tension; Plateau channels

1 Introduction

Foams includes two phases of gas and liquid, along with the surfactant molecules in the liquid which reduce the surface tension of the liquid at the liquid-gas interface to facilitate foam formation. As shown in Figure 1, the liquid volume fraction,Ø may vary from less than 1% (dry foam) to around 36% (wet foam) under gravity effect [1]**.** Typically, foam channels are divided into internal channels and external channels. The internal channels can be considered as flow through a collection of long channels that are called Plateau borders (PB) and junctions of four PBs that is called node. The external channels' fundamental difference with internal channels is the existence of a no-slip wall[2]. However, foams are often inside of containers and has one side in contact with air, so it is necessary to classify the foam channels more comprehensively. In this study, the foam channels that come into contact with air are called the open channels, and the wet foam channels are discussed and studied emphatically.

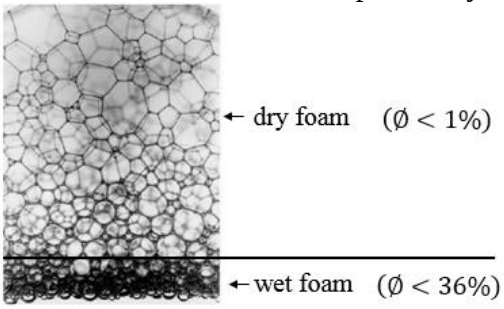

Figure 1. Foam gas-liquid two-phase distribution

Foams have numerous applications in the industries, agriculture and food. Industrially, their ability to preferentially gathering desired materials has made them greatly useful in the mineral industry for collecting desirable elements, and they can also be used for crop spraying in agriculture. These successful applications of foam rest on the capability of water-based foam to distribute a small volume of liquid over a wide area[2][3][4]. Therefore, one of the major question about the dynamical behavior of foams is the forming process of liquid channel structure in foams. Understanding the factors that influence bubbles' behavior such as surfactant materials and the forming process of different kinds of channels structure in foam is crucial in increasing its efficiency for current applications as well as creating potential new applications for foams. To better understand the factors that influence bubbles' behavior and the formation mechanism of various foam channel structures, requires a more complete description and study of the flow behavior and different kinds of foam channel structure respectively.

Along with the extensive application of foams in many aspects, great progress has been made in making the science of foams a sound including theories models, numerical simulation methods and experiments respectively. Hot topics have included static structure (the shapes and arrangements of bubbles), and dynamic evolution such as coarsening due to diffusion of gas, capillary and gravity driven drainage, rheology and coalescence due to rupture of the films [1][5][6]. Koehler et al. expanded the basic microscopic model by a theoretical study and experimental investigations at the scale of a single Plateau border for the flow rates, obtaining experimental results of velocity profiles inside the both interior and exterior PBs[2][7]. D. G. T. Barrett et al. employed experiments to help us to understand the dynamics of foam instability, and static (or quasi-static) simulations using the Surface Evolver to establish equilibrium film shapes in different frame shapes and sizes[8]. Besides, in gravity environment, the hydrodynamic process will result in uneven distribution of liquid film thickness from top to bottom. At the same time, the rapid liquid loss also makes it difficult for the bubbles to evenly and stably distribute in the foam. However, the buoyancy disappears and gravity drainage is suppressed under low microgravity, capillary drainage is slowed down due to the quasi-spherical shape of the bubbles, so the overall behavior of foam will show completely different characteristics from that under normal gravity. The microgravity environment of 20~25 seconds (0.01G) was realized by parabolic aircraft flight method, and then the liquid evolution process of two-dimensional foam was observed and analyzed, but these experiments are relatively isolated and their results are not well analyzed[9].

There have been many numerical method of the foam in recent years. Among the approaches, VOF[10] and level set method[11] are applied extensively. In fact, the VOF method tracks the volume fraction of each phase or component instead of tracking the interface itself. The interface is reconstructed from the values of volume fraction which imply that it would be complicated for VOF to be extended to the three-dimensional case. For the level set method, it uses the level set function to store the information of the interface. The advantage is that the level set function varies smoothly across the interface while the volume fraction is discontinuous. Besides, the curvature can be easily evaluated from the level set function. However, the level set method requires a re-initialization procedure to keep the distance property when large topological changes occur around the interface. This may violate the mass conservation for each phase or component. The LBM method [12] was also applied to study the deformation of a single bubble or several bubbles in the liquid, but the surface tension force acts only on the single-gas-liquid-interface in the liquid.

Most studies focused on the bubble's shape and deformations in the liquid or the tube where the surface tension force acts only on the single-gas-liquid-interface in the liquid. And most of

the mentioned studies' numerical models are two-dimensional simulation which are suitable for the specific individual parts of foam, whereas a three-dimensional model can overcome the shortcomings of two-dimensional simulation by analyzing the overall structure of foam. Besides the study of wet foams is essential to understand and control foaming processes. However, foams are created in a transient wet state and evolve rapidly afterwards under normal gravity. Indeed, a micro- or zero-gravity study of wet foam hydrodynamics removes the various instabilities experienced under normal gravity, but these experimental methods are difficult to achieve, or the weightlessness time is too short, or the preparation cycle is too long, resulting in scattered experimental research results in this field. All these questions have motivated the use of numerical methods to carry out wet foam investigations without considering the gravity effect.

To model the behavior of a single film bubbles with double-gas-liquid-interfaces in the absence of gravity, two main issues including surface tension force modeling and interface recording have to be considered. The moving particle semi-implicit (MPS)[13] is employed in this study because of the advantage in dealing with the large deformation. So far, the MPS method was successfully used in engineering and science, such as the deforming process of bubbles in the air[14], and the multiphase flows with deformable interfaces movement[15]. Figure 2 is the schematic diagram of the framework of this study. The aim of this study is to present a three-dimensional model for the foam system including interior node-PB and exterior node-PB as well as open node-PB without considering the effect of gravity. Firstly, the factors of the effect on the dynamic behavior of bubbles including surface tension coefficient and fluid viscosity were studied respectively to present a comprehensive comparison on foam behavior in the presence of various physical conditions and bubble sizes. Subsequently, the forming process of different kinds of foam channel structure were displayed and discussed. Once the forming process of different kinds of foam channels structure including exterior and interior as well as open channels were studied, a complete geometrical model for the foam can be used in foam stability study in different environments. This study is anticipated to broaden the recognition of the foam behavior and the formation mechanism of various foam channel structures without considering gravity.

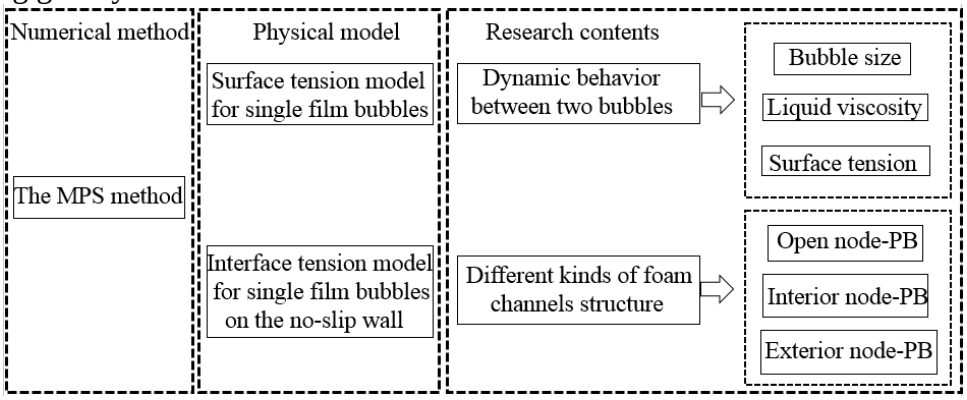

Figure 2. Schematic diagram of the framework

2 Numerical method

2.1 The MPS method

In the MPS method, the governing equations of the flow mechanics include the conservation equations of the mass and the momentum. For an incompressible flow, they can be written in a Lagrangian form as:

$$\frac{D\rho}{Dt}+\rho\nabla\cdot\boldsymbol{u}=0 \tag{1}$$

$$\rho \frac{\mathrm{D}\boldsymbol{u}}{\mathrm{Dt}} = -\nabla P + \mu \nabla^2 \boldsymbol{u} + \rho \boldsymbol{f} \tag{2}$$

where ρ is density, t is time, $\boldsymbol{u}$ is velocity, P is pressure, μ is dynamic viscosity coefficient, $\boldsymbol{g}$ is acceleration of gravity, and $\boldsymbol{f}$ is the volumetric force, such as gravity and surface tension force, ∇ is gradient, ∇^2 is Laplacian. The calculation area and its boundary are discretized by a set of particles, which are divided into three kinds including fluid particles, gas particles and solid particle with different physical parameters in this study. The interaction between adjacent particles is defined by a kernel (weight) function:

$$w(r) = \begin{cases} \frac{r_e}{r} - 1 & (r \le r_e) \\ 0 & (r > r_e) \end{cases} \tag{3}$$

Where r is the distance between the two particles. This effective radius r_e is $2.1l_0$, and l_0 is the initial distance between two neighboring particles. It is obvious that the kernel function is only valid within the effective radius. Similar to the physical density of the liquid, a particle density is defined as:

$$n_i = \sum_{j \ne i} w(r) \tag{4}$$

It is a constant value n_0 for an incompressible fluid but a little smaller on the free surface. Any movement of the particles would change the particle density to a temporal n_i^*. In order to modify it back to n_0, the pressure is calculated by solving the Poisson equation with Incomplete Cholesky Conjugate Gradient (ICCG) method:

$$\langle \nabla^2 P^{n+1} \rangle_i = \frac{\rho}{\Delta t^2} \frac{\langle n_i^* \rangle - n_0}{n_0} \tag{5}$$

By treating the foam system as a multi-density multi-viscosity fluid, the mesh-free particle method for incompressible multiphase flow has been introduced in this study based on the MPS. At the interface, a particle with viscosity μ_1 (or density ρ_1) may interact with particles with viscosity μ_2 (or density ρ_2). The multi-viscosity and multi-density models are derived from the interaction between particles with different properties.In this study, the harmonic mean viscosity model is used to calculate the viscous momentum transfer process.

$$\frac{1}{\rho} \nabla \cdot (\mu \nabla \varphi) = \frac{2d}{\rho_i \lambda n_0} \sum_{j \ne i} \left[\frac{2\mu_i \mu_j}{\mu_i + \mu_j} (\varphi_j - \varphi_i) w(|\boldsymbol{r}_j - \boldsymbol{r}_i|) \right] \tag{6}$$

where φ is an arbitrary scalar, d=3 indicates a three-dimensional problem. Similar to the harmonic mean viscosity model, the harmonic average method is applied to the average density model so that the change of pressure field in the transition region was relatively gentle. In this way, the pressure field distribution in the transition region is conducive to ensuring the stability of the simulation. Poisson equation of pressure can be written as:

$$\nabla \cdot \left(\frac{1}{\rho} \nabla P \right) = \frac{2d}{\lambda n_0} \sum_{j \ne i} \left[\frac{P_j - P_i}{2\rho_i \rho_j / (\rho_i + \rho_j)} w(|\boldsymbol{r}_j - \boldsymbol{r}_i|) \right] \tag{7}$$

After obtaining the distribution of the multiphase pressure field, the following pressure gradient model was used to calculate the pressure gradient term:

$$\nabla P = \frac{2d}{n_0} \sum_{j \ne i} \left[\frac{P_j + P_i}{|\boldsymbol{r}_j - \boldsymbol{r}_i|^2} (\boldsymbol{r}_j - \boldsymbol{r}_i) w(|\boldsymbol{r}_j - \boldsymbol{r}_i|) \right] \tag{8}$$

Only brief outline of the MPS method is given in this section, more detailed models and algorithms could be found in relative references[13].

2.2 Surface tension model

According to the single film bubble's geometric feature (Figure 3), it could be considered as a liquid film shell with an amount of gas on both sides in the air. Since the flow of the liquid film and the deformation of the bubble often happen in a very low Reynolds Number with a very small velocity, the gas outside of the bubble is assumed that it has a very limited influence on the bubble. In the algorithm of the MPS, the influence of the outside gas on the bubble will be totally ignored except as the atmosphere pressure in this study. In other words, there will be no gas particles in the gas phase outside the bubble system, and we have zero pressure constantly on the outside free surface open in the air, but both sides of the film formed between bubbles are affected by gas.

Though the single liquid film is very thin, it has two gas-liquid interfaces including outside interface and inside interface. In order to accurately calculate the surface tension force on both sides, an interlayer of viscous fluid particles is employed to represent the liquid between the two interfaces. On the other hand, the gas inside the bubble is taken as incompressible and has a uniform density and pressure so that the surface tension force which acts on both sides of the film formed between bubbles in foams can be calculated.

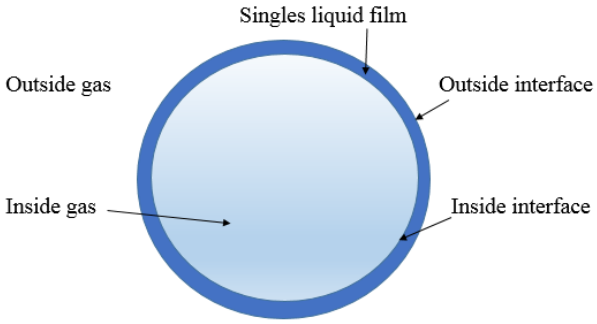

Figure 3. The geometric feature of single film bubble

Within the framework of the MPS method, the surface tension forces on the two interfaces will be calculated integrally using the surface free energy surface tension model[16]. The potential energy between two particles is denoted by P(r), and then the force $\boldsymbol{f}$ between the particles is:

$$\boldsymbol{f} = \frac{\partial \mathrm{P}}{\partial \mathrm{r}}\boldsymbol{n} \tag{9}$$

According to the requirement of repulsion when the distance between particles is less than a critical value and attraction when it is larger than a critical value. The force between the particles can be calculated by different formulas[16]**.** For the particles with particles of uniform and symmetrical distribution around, the resultant force on them is 0, when the particles are on or adjacent to the free surface, the resultant force is not 0, that is the surface tension. Therefore, the formula for calculating the potential energy between particles is[17]:

$$P(r) = \begin{cases} \frac{1}{3}C\left(r - \frac{3}{2}l_{min} + \frac{1}{2}r_e\right)(r - r_e)^2 & (\mathrm{r} < r_e) \\ 0 & (r \geq r_e) \end{cases} \tag{10}$$

where C is a modified parameter, which can be obtained according to the physical properties of fluids. l_{min} is the boundary of repulsion and attraction, which is also the extreme point of surface free energy. l_{min} is $1.5l_0$, and r_e is $3.1l_0$ in the subsequent numerical calculation and research[18].

2.3 Interface tension

When the foam contacts the container, the external channels are created. For small foam containers, the relative number of exterior and interior channels is significant. Therefore, it is necessary to study the formation mechanism and the factors influencing the formation of external channels.

Interface tension exists between different substances that are in contact but not mutually soluble such as liquid-gas, liquid- liquid and liquid-solid. The wetting effect between multiple interfaces can be described by the following equations[18]:

$$\begin{cases} \sigma_{\alpha\theta}cos\alpha + \sigma_{\alpha\beta} + \sigma_{\beta\theta}cos\beta = 0 \\ \sigma_{\alpha\theta} + \sigma_{\alpha\beta}cos\theta + \sigma_{\beta\theta}cos\beta = 0 \\ \sigma_{\alpha\theta}cos\alpha + \sigma_{\alpha\beta}cos\theta + \sigma_{\beta\theta} = 0 \\ \alpha + \beta + \theta = 360° \end{cases} \tag{11}$$

where α, β and θ are contact angles, $\sigma_{\alpha\theta}$, $\sigma_{\alpha\beta}$ and are the surface tension coefficients of non-gaseous contact material.

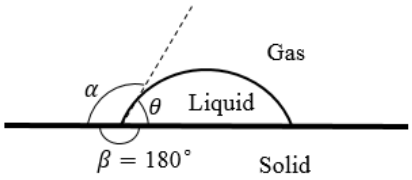

Figure 4. The relationship between contact angles and interface tensions

For the liquid-solid interface tension case, since the solid is considered as rigid body, β in Figure 4 is 180 °. Contact angle θ of liquid-solid system demonstrates the wettability of solid surface. If θ is smaller than 90 °, the solid surface is hydrophobic, or else the solid surface is hydrophilic. In this study, we focus on the effect of hydrophobic/hydrophilic solid surface on the forming process of the external channels.

3 Numerical validation

3.1 Oscillation of square single film bubble

The square single film bubble oscillation process is calculated with the surface tension model as a classic validation case. The results are shown in Figure 5. Initially, a square single film bubble is arranged with 60×60 particles including liquid particles and gas particles. The side length of the square bubble is 18 mm and the spacing between the particles is l_0=0.0003m. The time step is t = 0.00001s, and the physical parameters are shown in the captions of Table 1.

Table 1. Particle Physical property parameters

Material	Density（kg/m^3）	Dynamic Viscosity Coefficient（N·S/m^2）	Surface Tension Coefficient（N/m）
Water	1000	1.01×10^{-3}	0.0725
Gas	1.5	1.79×10^{-5}	—

The single film is composed of three layers of particles including the outside layer, the inside layer and the inter layer between them. The gas outside the bubble is ignored, and the gas inside the bubble is incompressible and uniform which is not shown in these figures (Figure 5).

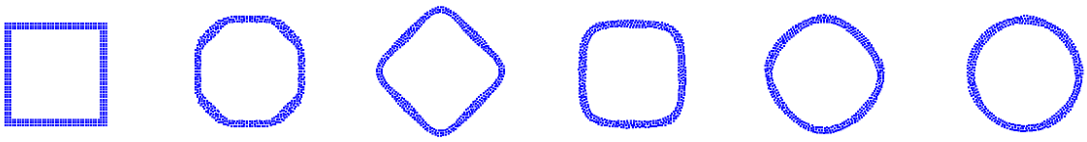

(a) t=0 s (b) t=0.02 s (c) t=0.04 s (d) t=0.08 s (e) t=0.2 s (f) t=0.86s

Figure 5. Oscillation process of square single film bubble under surface tension forces

The square bubble firstly shrinks from the four corners with large curvatures until it is deformed into a diamond shape. Then the similar deforming process repeats, the square shape and the diamond shape appear alternately. However, since the viscous dissipation of the liquid and the gas, their interaction reduce the energy gradually in every time step, and the oscillation amplitude shows damped oscillation attenuation with time. Finally, the deformation will end when the amplitude approaches zero in Figure 6. As a result, a perfect round shape (t = 0.86 s in Figure 5) is generated.

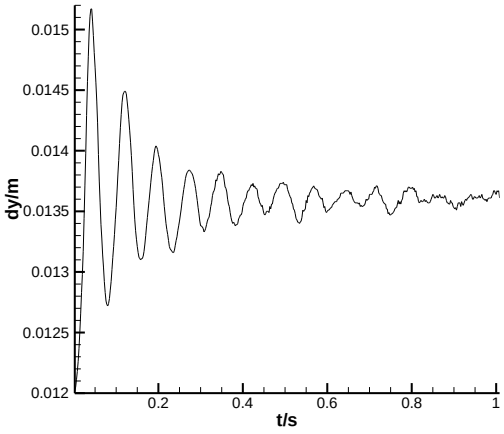

Figure 6. Amplitude variation curve of y-axis oscillation during bubble deformation

The square single film bubble oscillation process is a benchmark test to verify surface tension model. We know that Laplace law for the two-dimensional case is[19]:

$$\Delta P = \frac{\sigma}{R} \tag{12}$$

Where ΔP is the pressure jump across the interface. R is the radius of the bubble. When the amplitude approaches zero, ΔP can be calculated by counting the average pressure o the liquid film with the corresponding bubble radius R. The radius is set to be 3, 4, 5, 6, 7 and 8mm respectively. The surface tension coefficient σ is taken as 0.072N/m. Then, the numerical results and the analytical solution (Eq. (12)) are drawn as a function of the radius of the bubble in Figure 7. As can be seen from the Figure 7, the numerical results agrees well with the analytical solution. These show that the Laplace law is accurately satisfied.

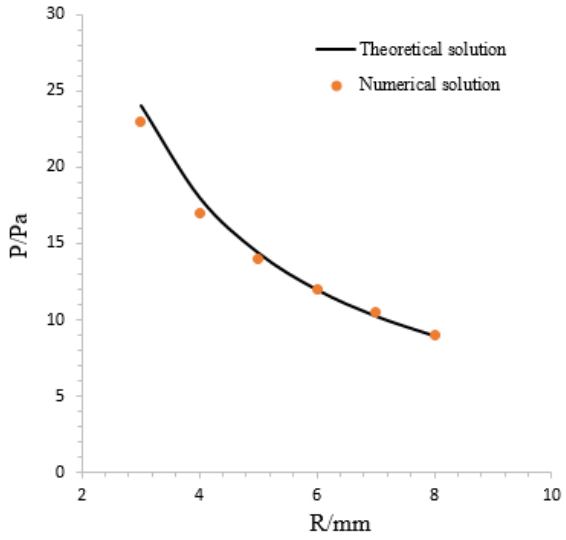

Figure 7. The verification of Laplace law

3.2 The solid-liquid wetting effect

A two-dimensional water droplet wetting on a solid wall without gravity was simulated in this section to verify the interface tension mentioned above. Theoretical solutions exist for a droplet wetting on solid under zero gravity as shown in Figure 8. The stable contact angle θ is formed at the contact point between the three phases[18]. Due to the surface tension, the free surface of droplet presents a regular sphere, and it's a regular arc in two-dimensional space. The relation of the parameters on Figure 8 is:

$$V=\pi R_0^2 = \frac{1}{2} \times 2\pi R \frac{2\theta}{2\pi} \times R - R\sin\theta \times R\cos\theta \quad (13)$$

$$S=2R\sin\theta \quad (14)$$

Where V is the volume of the droplet, S is the area of the contact part, R is the radius of the droplet surface,R_0 is the initial radius of the droplet.

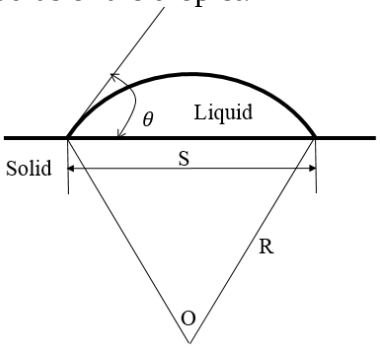

Figure 8. The relationship between contact angle and contact area in solid-liquid wetting

Figure 9 is the time serial of a water droplet wetting process on a solid wall under zero gravity with a static contact angle of 60°. The initial droplet radius is 0.02m with particle size l_0=0.001m and the time step is 0.001s. As shown in Figure 9, the wetting length increases rapidly with time, and the dynamic contact angle and droplet height decrease gradually.

(a) t=0 s (b) t=0.5 s (c) t=1.5 s (d) t=2 s (e) t=3 s (f) t=5 s

Figure 9. Droplet wetting process on a solid wall

As shown in Figure 9(f), the droplet reaches finally stable at about t=5s with steady contact angle and area like Figure 10.

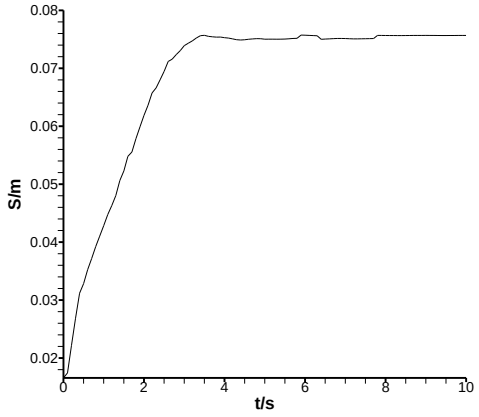

Figure 10. Curve of wetting length over time

Figure 11 shows the contact area of numerical and theoretical results at different contact angle. The simulation results indicate that the surface tension model and the interface tension mentioned could simulate solid-liquid wetting effect correctly.

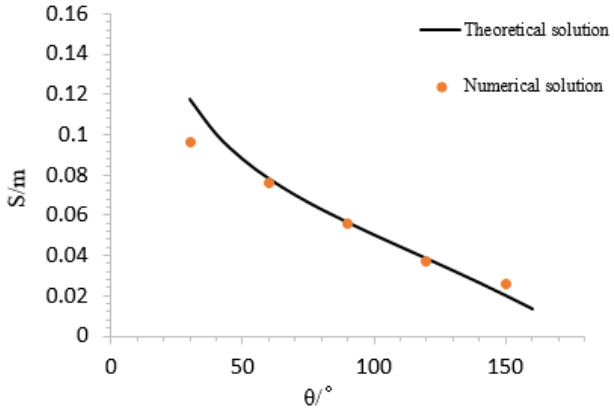

Figure 11. Contact area of numerical and theoretical results at different contact angle

4 Numerical simulation and discussions

4.1 Dynamic Behavior Between Two Bubbles

In order to study the dynamic behavior of bubbles in detail, the flow field velocity of the liquid film in the calculation area is counted, and the average velocity of the liquid film is obtained from the following formula.

$$velo_L = \frac{\sum_i^{N_L} velo_i}{N_L} \tag{15}$$

Where $velo_L$ is the average velocity of liquid film particles, N_L is the total number of liquid particles, $velo_i$ is the velocity of liquid particle i.

Without considering the effect of gravity, the process of bubble coalescence at the same scale is simulated and the effects of different physical parameters on its dynamic behavior are analyzed. Then the more general phenomenon of bubbles' dynamic behavior at different scales is simulated and analyzed.

4.1.1 Simulation of interaction between the same sizes of single film bubbles

Figure 12 is the time serial of the coalescence process of three-dimensional bubbles with the same size. The initial position of the bubbles is shown in Figure 12(a), and Figure 12(b-f) is obtained by cutting along the plane of the center of two bubbles where blue particles and red particles represent liquid film and gas respectively. The radius of the bubble is 4.5 mm with particle size l_0=0.3mm, the distance between the center of mass of the bubble is 9.3 mm, the thickness of the liquid film is 0.9 mm, and the time step is 0.00001 s. The physical parameters are shown in the table 2.

Table 2. Particle Physical property parameters

Material	Density （kg/m^3）	Dynamic Viscosity Coefficient（N S/m^2）	Surface Tension Coefficient（N/m）
Water	1000	2×10^{-2}	0.032
Gas	1.5	1.79×10^{-5}	—

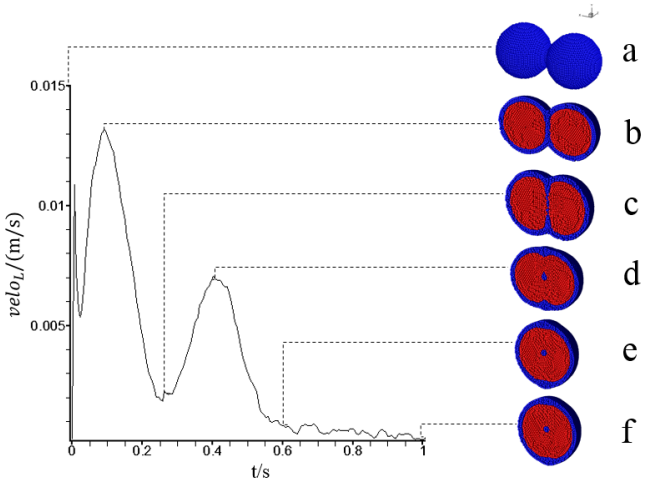

Figure 12. The coalescence process of three-dimensional bubbles with the same size

It can be seen from the Figure 12 that the initial velocity of two equal-scale bubbles is zero at the initial time. Since the bubble is not a sphere in the strict sense when it is arranged in Cartesian coordinates, the bubble shrinks into a sphere under the action of surface tension .Therefore, the average velocity of liquid film increases sharply in a very short time .In the process of forming spheres, two bubbles contact each other (there is a small degree of extrusion), and liquid film is formed between bubbles, then the average velocity of liquid film decreases sharply. The above process takes place in a very short time and can be regarded as an adaptive process of the initial physical environment of bubbles, so the influence of fluid properties on this stage can be neglected.

In the initial stage (a-b) of the contact process between two bubbles, a large curvature is formed at the angle between the outside of the liquid film. The surface tension drives the surface of the liquid film to deform and fuse rapidly, which makes the average velocity of liquid film increase.

With the continuous approaching of bubbles (b-c), the average velocity of liquid film decreases because the squeezing degree between bubbles increases. Besides, the intermediate liquid film gradually expands to both sides so that the liquid film becomes thinner through continuous drainage.

Subsequently, under the action of inertia, bubbles continue to move toward the center (c-d) and the liquid film breaks up when the liquid film thickness reaches a critical value. Because the liquid film formed between bubbles is not uniform, there is a curvature difference, the liquid film gradually stretches longitudinally, and the average velocity of liquid film shows an upward trend.

When the liquid film is stretched to a certain extent, it gradually shrinks to the center (d-e) under the action of surface tension with ellipsoidal bubbles transiting to spherical bubbles. Finally, under the action of surface tension and viscous dissipation, the average velocity of liquid film also shows a trend of attenuation through continuous contraction oscillation.

Finally, the oscillation amplitude becomes smaller and smaller, and the average velocity of liquid film basically remains unchanged, and approaches zero. The two bubbles merge into a large bubble with a stable shape (e-f).

Besides, the broken liquid film disperse in the bubble without the gravity, and under the action of surface tension, the small spherical droplet are formed. Because of the symmetry, the small spherical droplet suspends in the center of the bubble.

4.1.2 The influence of different physical parameters on the interaction between bubbles

From the above analysis, it can be found that when bubbles merge, the velocity curve shows damping oscillation attenuation with the shape of bubbles changed. Finally, the average velocity of liquid film becomes zero, and the two bubbles merge into a static spherical bubble. From the point of view of energy, the two bubbles are driven by chemical potential energy in a static state with a tendency to form a bubble. The shape of bubble deforms during coalescence, which will cause viscous dissipation and consume a part of energy. The chemical potential energy is related to the surface tension of bubbles, so the effects of surface tension and fluid viscosity on the dynamic behavior of bubbles will be studied below.

For the coalescence process of three-dimensional bubbles with the same size above, Figure 13 is the average velocity of liquid film under different viscous coefficients with the same surface tension coefficient, and other parameter settings are the same as table 2 except for the dynamic viscosity coefficient.

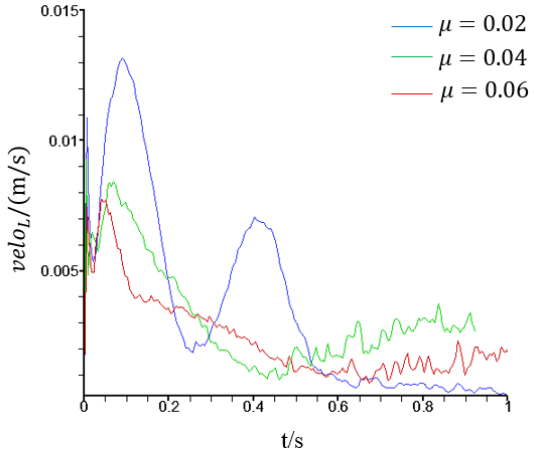

Figure 13. Average velocity of liquid film under different viscous coefficients

The smaller the viscous coefficient is, the larger the first peak value of the bubble coalescence speed and the larger the oscillation amplitude of the velocity curve are, which shows that the

chemical potential energy in the process of bubble coalescence is dissipated through the viscous term. The larger the viscous coefficient is, the more the energy dissipation per unit time is. With the increase of viscosity, the peak velocity of liquid film decreases, and the time required to reach the first peak velocity decreases.

With the increase of viscous coefficient, the deformation of bubbles is smaller in unit time. This is precisely because the viscous coefficient reflects the strong degree of fluid impediment to bubble motion. If the viscous coefficient is large, the resistance of the bubbles' coalescence will be large, and the viscous dissipation will be large in the course of motion. Therefore, the larger the viscous coefficient is, the less likely the liquid film held by the bubbles in the interaction will crack.

Similarly, Figure 14 is the average velocity of liquid film under different surface tension coefficients with the same dynamic viscosity coefficient, and other parameter settings are the same as table 2 except for surface tension coefficient.

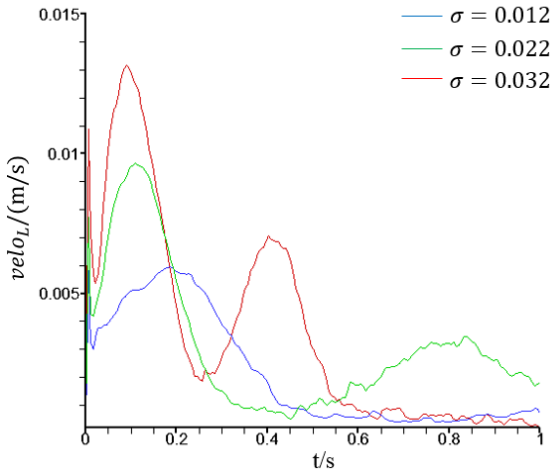

Figure 14. Average velocity of liquid film under different surface tension coefficients

The relationship between the first peak value of velocity and surface tension is opposite to that of viscosity. The higher the surface tension is, the earlier the bubbles begin to polymerize, and the higher the average peak velocity of liquid film is.

With the increase of surface tension, the deformation of bubbles increases in unit time, which shows that the chemical potential energy is related to the surface tension of bubbles. Under the effect of surface tension, the surface free energy of bubbles changes into kinetic energy, and the average velocity of particles increases.

4.1.3 Simulation of interaction between the different sizes of single film bubbles

It can be seen from the above analysis that when the viscosity coefficient is increased or the surface tension is reduced, the stable shape of the connection between bubbles is more likely to appear. The new physical parameters are shown in the table 3. Figure 15 is the time serial of the connection process of three-dimensional bubbles with the different sizes. The initial position of the bubbles is shown in Figure 15(a). The radius of the bigger bubble is 6 mm and the radius of the smaller bubble is 3 mm with particle size l_0=0.3mm, the distance between the center of mass of the bubble is 9.3 mm, the thickness of the liquid film is 0.9 mm, and the time step is 0.00001 s.

Table 3. Particle Physical property parameters

Material	Density（kg/m^3）	Dynamic Viscosity Coefficient（N S/m^2）	Surface Tension Coefficient（N/m）
Water	1000	2×10^{-2}	0.012
Air	1.5	1.79×10^{-5}	—

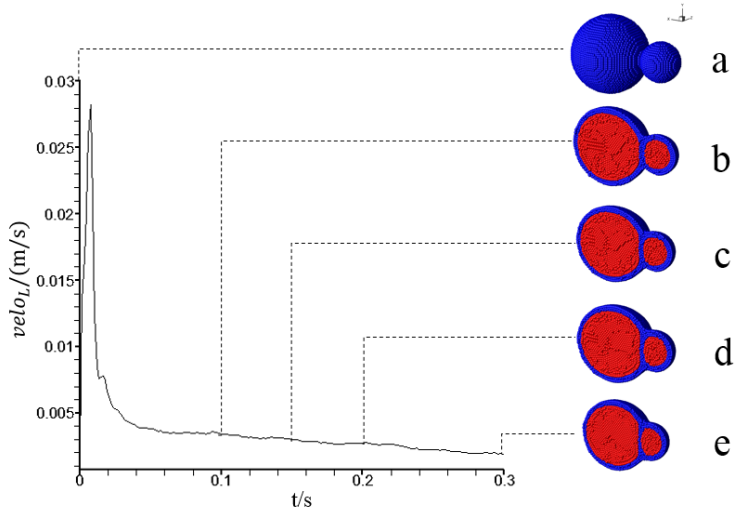

Figure 15. The connection process of three-dimensional bubbles with the different size

It can be seen from the Figure 15 that when the two bubbles start to contact each other at the beginning, the curvature of the place where the bubble contacts is large, and the liquid film is rapidly deformed and fused under the surface tension (a-c). Then, a liquid film is formed between the bubbles (c-e).

Due to the symmetry, the liquid film held by the two bubbles with the same size is a circular plane when they are in contact with each other. However, when the non-equal two bubbles are in contact with each other, the liquid film is a spherical surface having a certain curvature and is convex toward the larger bubble direction (d-e), because the small bubble curvature is larger than the large bubble, and the additional pressure of the small bubble is greater than the large one.

4.2 The forming process of different kinds of foam channels structure

By simulating the dynamic behavior of three-dimensional single-film bubbles of equal and non-equal scales, typical flow phenomena and deformation characteristics and rules of liquid film are obtained, and the effects of basic physical parameters including surface tension and dynamic viscosity on flow and deformation were studied. On the above basis, further research on the formation mechanism of various foam channel structures has been carried out through the following work.

To better understand the formation mechanism of various foam channel structures, requires a more complete description the different kinds of foam channel structure firstly. In liquid foam, bubbles stack with each other, and the gaps between bubbles form a network channel for the flow of trace liquid, which is composed of Plateau channel and the junction point. In this study,

the foam channels are divided into three types including interior node-PB and exterior node-PB as well as open node-PB. Subsequently, the forming process of different kinds of foam channel structure were displayed and discussed as follows.

4.2.1 Open node-PB

In the study of the open Plateau channel where the bubbles in the foam are in contact with the air, in order to save computing resources and ensure the rationality of the calculation results, three bubbles with the same size are selected as the basic unit of calculation.

Figure 16 is the time serial of a cross-section of three bubbles with the same size during connection and the gas inside the bubbles is not shown in the figures. The initial arrangement of three bubbles with the same size is shown at t = 0s, the radius of a single bubble is 6 mm, and the thickness of the liquid film is 0.9 mm. Under the action of surface tension, the three bubbles contact with each other, then the liquid film deform rapidly and stick together with each other. During this process like Figure 16(a-d), the liquid film held between bubbles expands continuously, and the space occupied by air between bubbles is filled by liquid film continuously. Finally, the liquid film held by the three bubbles does not change significantly, and form a more stable system like Figure 16(f). The liquid film in the stabilized bubble system shows good symmetry, and the angle between adjacent liquid films is about 60 °.

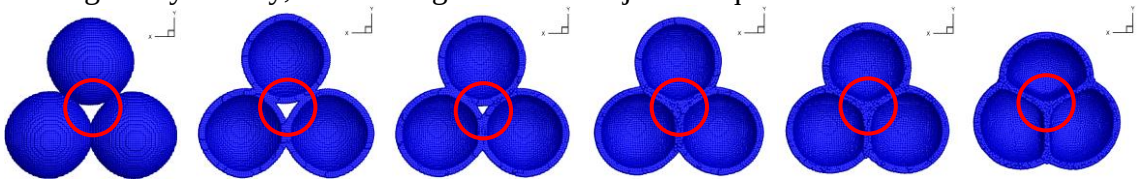

(a) t=0 s (b) t=0.02 s (c) t=0.04 s (d) t=0.06 s (e) t=0.1 s (f) t=0.3 s

Figure 16. Three equal-scale bubbles connection processes

At the same time, in order to further study the details of bubble evolution from sphere to polyhedron, triangle in polygon configuration is selected as the basic research unit, and the process of gas disappearance and polygon formation is analyzed in Figure 16(a-f) where the part marked with red circles. At the initial moment, the bubble is completely circular, and the gas in the triangle region is the largest. With the structure evolution of adjacent bubbles under surface tension, the triangular region begins to sew up and the internal gas decreases gradually. At t=0.3 s, all the gas disappear with the curved surface held by bubbles gradually becoming flat. At this time, it can be predicted that when the space is filled with multiple bubbles, the polygon structure can be formed completely.

In order to better analyze the formation mechanism of liquid film channel for micro-liquid flow in the process of bubble interaction, the channel structure at a specific time is specially extracted in this study.

Figure 17 is the time serial of three bubbles forming an Open node-PB during the connection process. Under the action of surface tension, bubbles keep approaching each other, and the space occupied by air between bubbles is continuously filled by liquid film. Each bubble liquid film contacts with each other to form a new liquid film and a liquid film channel encapsulating the liquid film. Later, the distance between bubbles decreases further, and the area of liquid film held by bubbles enlarges and the channel of liquid film encapsulating liquid film increases. When the channel of liquid film increases to a certain extent, the channel of liquid film contacts with each other to generate a new liquid film channel and two nodes. As shown in Figure 17(a-

e), there is no independent channels which are connected by nodes. Each node has four channels, and the channel centered on the nodes is umbrella-shaped. If the formation mechanism of a single node is analyzed, the basic process is similar to the above process. It is very similar to the formation of the liquid film channel and the nodes between the channels in the foam system, which is directly contacted with the air. Therefore, this type of channel is an Open node-PB in this study.

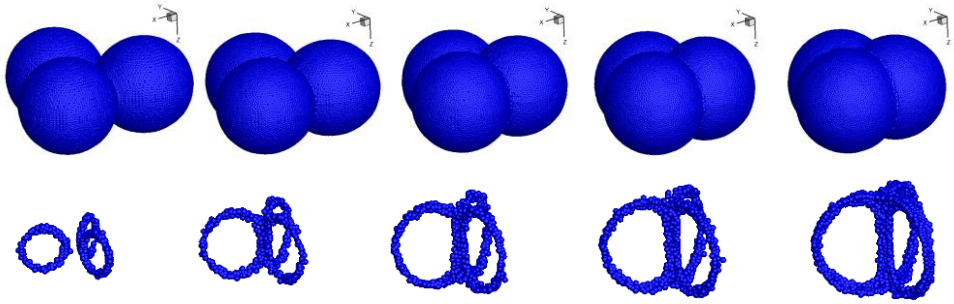

(a) t=0.05 s (b) t=0.1 s (c) t=0.15 s (d) t=0.2 s (e) t=0.3 s

Figure 17. Three equal-scale bubbles connection processes with film channels

4.2.2 Interior node-PB

Similarly, in the study of the internal Plateau channel in the foam system, in order to save computing resources and facilitate the analysis and discussion of the formation of the internal Plateau channel, four bubbles with the same size are selected to form a basic unit of interaction in this study.

Figure 18 is the time serial of formation of Plateau Channels in four bubbles during the connection process. Initially, the four bubbles are tetrahedral distribution. The radius of a single bubble is 6 mm, and the thickness of the liquid film is 0.9 mm. Under the action of surface tension, the four bubbles contact each other, and make the liquid film rapidly deform and bond with each other. In this process, the liquid film held by the bubbles expands continuously, and the space occupied by the air between bubbles is filled and occupied by the liquid film continuously. Finally, the liquid film held by the four bubbles does not change significantly, and form a relatively stable system, which is similar to the behavior of the three bubbles mentioned above.

As bubbles keep approaching each other, six new liquid films and the liquid film channels encapsulating the liquid membranes are formed. When the liquid film channel increases to a certain extent, the liquid film channel contacts each other, and four new liquid film channels are generated and five nodes are generated. This paper considers that the external liquid film channel (outline) is a part of the interaction between the basic unit and other basic units, so it is neglected in the discussion.

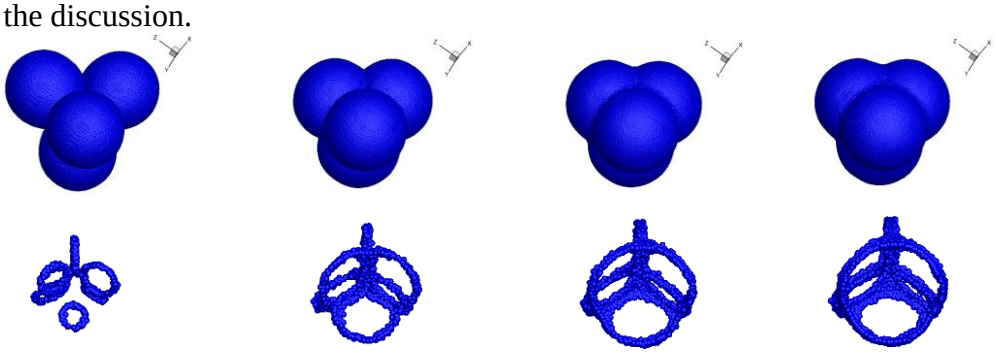

(a) t=0.05 s (b) t=0.15 s (c) t=0.3 s (d) t=0.45

Figure 18. Four equal-scale bubbles connection processes with film channels

In order to better analyze the channel structure, the internal Plateau channel at t=0.45 s is specially extracted and rotated every 60 degrees along the x-axis in this study. As shown Figure 19 below, the four bubbles share a central interior node, where each of the three bubbles forms a concave triangular inner Plateau border, and the four bubbles form four inner Plateau channels.

Figure 19. Interior node-PB structure at different angles

Figure 20 is the internal structure of four bubble stabilization units, where the different colors represent the different pressure values. As can be seen from the figure 20, the pressure values at channels and nodes are all higher than the pressure values of the nearby liquid film. The area with a smaller pressure value means the thickness of the liquid film there is smaller, in other words, it contains less liquid.

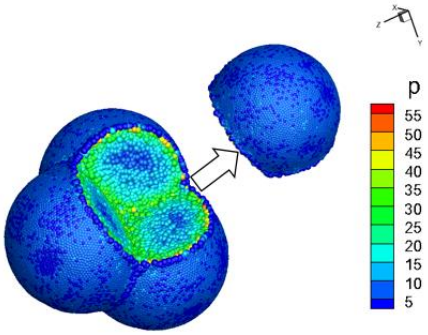

Figure 20. Internal structure of four bubble stabilization units

Figure 21 is the Plateau structural unit. For the whole foam system, the liquid is mainly distributed in the liquid films and liquid film channels, and the liquid content in the liquid film channels is more. If gravity is taken into consideration, the liquid stored in the liquid film channels will naturally drain, making it difficult for the entire foam system to remain stable for a long time. This is also one of the difficult problems in the experimental study of the formation mechanism and structural characteristics of the foam channel. In this section, the influence of gravity is neglected and the drainage process is suppressed, making the bubble system easier to achieve and maintain stable state. After considering the size of bubbles and the number of bubbles, the formation mechanism and structural characteristics of the whole foam system can be further analyzed.

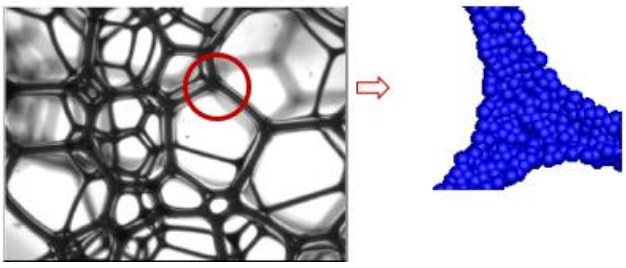

Figure 21. Plateau structural unit

4.2.3 Exterior node-PB

Foam systems usually exist in containers. Therefore, the relative number of exterior and interior channels is significant for small foam containers. The container wall is treated as flat wall in

this paper. The exterior foam's fundamental difference with interior foam is the existence of a no-slip wall.

The influence of vessel wall on channel formation is mainly in two aspects. One is that the existence of the wall restricts the space expansion of the channel to the normal direction of the wall during the formation process. The other is that the different wettability of the wall material to the liquid will affect the formation of the channel and the shape of the stable channel. In this study, the interaction of two bubbles on a flat plate with different wettability is simulated, and the effect of wall surfaces with different wettability on the formation of the channel and the shape of the stable channel is studied.

In order to facilitate the observation and analysis of the formation of external channels, the bubbles are split vertically along the center of the bubbles. Figure 22 is the time serial of the two bubbles interacting and infiltrating on a plate wall under zero gravity with a static contact angle of 30 °. The initial arrangement of two bubbles with the same size is shown at t = 0s, the radius of a single bubble is 3 mm, and the thickness of the liquid film is 0.9 mm. and the time step is 0.00001s.

As shown in Figure 22(a-d), the coalescence of two bubbles is accompanied by the infiltration of bubble liquid film into a flat plate. During the coalescence of the two bubbles, as the liquid film continuously infiltrates the wall, the bubble liquid film begins to contact the wall surface and connect with each other, and the liquid film held between the two bubbles undergoes the process of forming, expanding and breaking up like Figure 22(a-d). Then, the two bubbles coalesce into a larger bubble. Under the action of gas pressure and interfacial tension in the larger bubble, the liquid film in contact with the plate in the bigger bubble changes constantly and cracks finally like Figure 22(c-e). Subsequently, the fractured liquid film gathers on the plate to form an external channel in Figure 22(e-g). As shown in Figure 22(g-h), the external channel reaches finally stable at about t=0.35s with steady contact angle and area finally.

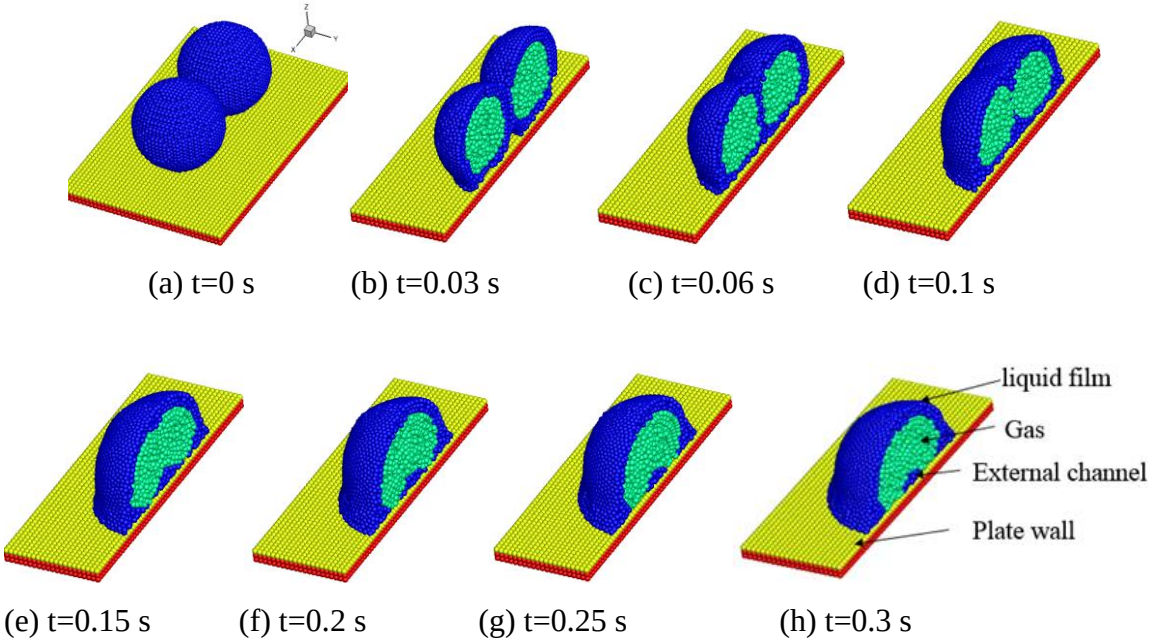

(a) t=0 s (b) t=0.03 s (c) t=0.06 s (d) t=0.1 s

(e) t=0.15 s (f) t=0.2 s (g) t=0.25 s (h) t=0.3 s

Figure 22. Bubbles wetting process on a solid wall

Figure 23 shows the axial cross section shape of the coalesced bubbles at different contact angles (30 °, 60 °, 90 °, 120 ° and 150 °), when the coalesced bubbles are in stable state on the plate. From the simulation results, it can be concluded that the different wall wettability will

affect the dynamic behavior of bubbles on the flat plate when bubbles are in contact with a flat plate. When the wall wettability is hydrophilic, it is easy to produce an exterior node-PB during the coalescence of multiple bubbles on a flat plate, and the shape of the axial cross section of the channel is closely related to the hydrophilicity. On the contrary, when the wall wettability is hydrophobic, it is hard for bubbles to form an exterior node-PB in the process of coalescence on the plate, but to spread a layer of liquid film on the plate, and the spreading area of the liquid film on the plate is related to the hydrophobicity. The stronger the wall hydrophobicity, the smaller the spreading area of the liquid film on the plate.

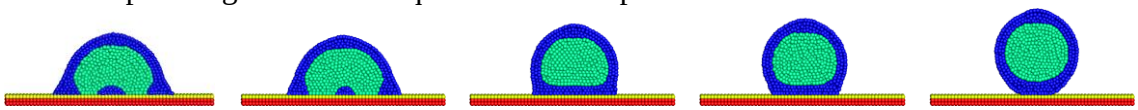

θ=30 ° θ=60 ° θ=90 ° θ=120 ° θ=150 °

Figure 23. Bubbles wetting result on a solid wall with different contact angles

5 Conclusions

Based on the MPS method, the bubbles behavior and the forming process of different kinds of foam channel structure were simulated in three-dimensional space by introducing the surface tension and interfacial tension model. The MPS method is a Lagrange method which avoids the occurrence of convection terms in the flow control equation, and eliminates the numerical dissipation phenomenon that may occur in the Euler method. The modeling process is more reasonable and the physical meaning of the parameters is clear, which provides a new idea for the study of foam dynamics .The main conclusions of this study are as follows.

By simulating the dynamic behavior of three-dimensional single-film bubbles of equal and non-equal scales, typical flow behaviors including coalescence and connection, and deformation characteristics and rules of liquid film are obtained. The effects of basic physical parameters on flow and deformation were studied. It was found that decreasing the surface tension coefficient or increasing the viscous coefficient would weaken the dominant role of surface tension in bubble deformation. As the simulation progresses, the bubble motion tends to be stable due to viscous dissipation.

Further, the Plateau channel structure in the foam system is further classified. The liquid channels in the foam system are divided into interior node-PB and exterior node-PB as well as open node-PB. The formation of different kinds of the Plateau channel structure is simulated and the results of each simulation are analyzed and discussed.

With the continuous approaching of bubbles, the length and cross-sectional area of channels formed between bubbles are increasing. Finally, when the multi-bubble system is stable, the main characteristics of liquid film channels are as follows:

For the open node-PB, there is no independent channels which connected by nodes. There are two nodes. Each node has four channels, and the channel centered on the nodes is umbrella-shaped. For the interior node-PB, the four bubbles share a node, where each of the three bubbles forms a concave triangular inner Plateau border, and the four bubbles form four inner Plateau channels. For the exterior node-PB, the different wall wettability will affect the dynamic behavior of bubbles on the flat plate when bubbles are in contact with a flat plate. When the wall wettability is hydrophilic, it is easy to produce an exterior node-PB during the coalescence of multiple bubbles on a flat plate, and the shape of the axial cross section of the channel is closely related to the hydrophilicity. On the contrary, when the wall wettability is hydrophobic,

it is hard for bubbles to form an exterior node-PB in the process of coalescence on the plate, but to spread a layer of liquid film on the plate, and the spreading area of the liquid film on the plate is related to of hydrophobicity. The stronger the wall hydrophobicity, the smaller the spreading area of the liquid film on the plate.

References

[1] D. Weaire, S. Hutzler, The Physics of Foams, Oxford University Press, Oxford, 2000

[2] S.A. Koehler, S. Hilgenfeldt, H.A. Stone. (2004) Foam drainage on the microscale I. Modeling flow through single Plateau borders, Journal of Colloid and Interface Science 276, 420–438.

[3] R.K. Prud'homme, S.A. Khan (Eds.), Foams, Theory, Measurements and Applications, Dekker, New York, 1996.

[4] L.J. Gibson, M.F. Ashby, Cellular Solids, Cambridge University Press, Cambridge, UK, 1997

[5] P. Stevenson (Editor), Foam Engineering: Fundamentals and Applications (Wiley, 2012).

[6] I. Cantat, S. Cohen-Addad et al, Foams – Structure and Dynamics (Oxford University Press, 2013).

[7] S.A. Koehler, S. Hilgenfeldt, H.A. Stone, (2004)Foam drainage on the microscale II. Imaging flow through single Plateau borders, Journal of Colloid and Interface Science 276, 439–449.

[8] D. G. T. Barrett , S. Kelly E. J. Daly et al, (2008) Taking Plateau into Microgravity: The Formation of an Eightfold Vertex in a System of Soap Films ,Microgravity Sci. Technol, 20:17–22

[9] Noever DA. Foam fractionation of particles in low gravity[J]. Journal of Spacecraft and Rockets, 1994, 31(2): 319-322.

[10] C.W. Hirt, B.D. Nichols, Volume of fluid (VOF) methods for the dynamics of free boundaries, J. Comput. Phys. 39 (1981) 201–225.

[11] M. Sussman, E. Fatemi, P. Smereka, S. Osher, An improved level set method for incompressible two-phase flows, Comput. Fluids, 27(1998) 663–680.

[12] H.W. Zheng, C. Shu , Y.T. Chew, A lattice Boltzmann model for multiphase flows with large density ratio, Journal of Computational Physics 218 (2006) 353–371.

[13] Koshizuka S. Oka Y. Moving-particle semi-implicit method for fragmentation of incompressible fluid [J]. Nuclear Science and Engineering, 1996, 123(3): 421-434.

[14] Zhangguo Sun,Ni Ni,Yijie Sun,Gung Xi,Modeling of single film bubble and numerical study of the plateau structure in foam system ,China Ship Scientific Research Center.https://www.jhydrod.com/2018,30(1):79-86

[15] Guangtao Duana, Bin Chena,Seiichi Koshizukab, Hao Xiang.Stable multiphase moving particle semi-implicit method for incompressible interfacial flow,Comput. Methods Appl. Mech. Engrg. 318 (2017) 636–666

[16] Tartakovsky A M, Meakin P. Modeling of surface tension and contact angles with smoothed particle hydrodynamics[J]. Physical Review E, 2005, 72:026301.

[17] Kondo M, et al. A development of surface tension model using inter-particle force[A].Proceeding of Computational Engineering Conference[C],2006,19:337-338.

[18] Xiao Chen, Zhongguo Sun, Guang Xi. Numerical Investigation on Droplet Wetting Effect With the MPS Method ,Proceedings of the ASME 2014 4th Joint US-European Fluids Engineering Division Summer Meeting FEDSM2014 August 3-7, 2014, Chicago, Illinois, USA.

[19] H.W. Zheng, C. Shu , Y.T. Chew. A lattice Boltzmann model for multiphase flows with large density ratio, Journal of Computational Physics 218 (2006) 353–371.